Wind and Structures, *Vol. 27, No. 4 (2018) 235-245*
DOI: https://doi.org/10.12989/was.2018.27.4.235

Elastic analysis of arbitrary shape plates using Meshless local Petrov–Galerkin method

H. Edalati*[1] and B. Soltani[2]

[1]*Faculty of Mechanical Engineering, Jasb Branch, Islamic Azad University, Jasb, Iran*
[2]*Faculty of Mechanical Engineering, University of Kashan, Kashan*

(Received September 14, 2017, Revised January 12, 2018, Accepted January 27, 2018)

Abstract. In this study the stress analysis of orthotropic thin plate with arbitrary shapes for different boundary conditions is investigated. Meshfree method is applied to static analysis of thin plates with various geometries based on the Kirchhoff classical plate theory. According to the meshfree method the domain of the plates are expressed through a set of nodes without using mesh. In this method, a set of nodes are defined in a standard rectangular domain, then via a third order map, these nodes are transferred to the main domain of the original geometry; therefore the analysis of the plates can be done. Herein, Meshless local Petrov–Galerkin (MLPG) as a meshfree numerical method is utilized. The MLS function in MLPG does not satisfy essential boundary conditions using Delta Kronecker. In the MLPG method, direct interpolation of the boundary conditions can be applied due to constructing node by node of the system equations. The detailed parametric study is conducted, focusing on the arbitrary geometries of the thin plates. Results show that the meshfree method provides better accuracy rather than finite element method. Also, it is found that trend of the figures have good agreement with relevant published papers.

Keywords: Meshfree; Mindlin classical plate's theory; Lagrange method; weak form integral; MLPG

1. Introduction

One of the most important advances in the field of numerical methods was the development of the finite element method (FEM) in the 1950s. In the FEM, a continuous media with a complicated shape is divided into some elements. The individual elements are connected together by a topological map called a mesh. The FEM is a robust and thoroughly developed method, hence it is widely used in engineering applications due to its versatility for complex geometries and flexibility for many types of linear and non-linear problems(Liu and Gu 2005, Akgul *et al.* 2017).

However, the FEM has the inherent shortcomings of numerical methods that rely on meshes or elements that are connected together by nodes in a properly predefined manner. This approach suffers from some weaknesses including: a) high cost of gridding the problem domain, b) low accuracy of stresses calculation, c) difficulties in adaptive analysis, d) limitations in solving some problems (the ones with large deformation simulate crack growth and failure). The root of these problems is the use of elements or mesh in the formulation stage.

In recent years to conquer these difficulties, new computational methods were presented, which unlike the FEM, gridding of the domain is not required to solve a problem. These are called elementfree or meshfree (MFree) methods. In these methods, only a set of nodes which are distributed in the domain of the problem are used to solve the governing differential equations. The merits of MFree methods have absorbed many researchers in calculation mechanics and they have carried out a plethora of research in order to expand these approaches.

An MFree method is used to establish system algebraic equations for the whole problem domain without the use of a predefined mesh for the domain discretization. MFree methods use a set of nodes scattered within the problem domain as well as sets of nodes scattered on the boundaries of the domain to represent (not discretize) the problem domain and its boundaries. These sets of scattered nodes are called field nodes, and they do not form a mesh. Advantages of MFree methods in recent published literature made many researchers to study and develop such methods.

One of the earliest MFree methods were finite difference method (FDM) that were described in 1937 and 1938 Szafrana (2005). Another well-known MFree method is the Smoothed Particle Hydrodynamics (SPH), which was put forward in 1977; it was initially used for modeling astrophysical phenomena such as exploding stars and dust clouds that had no boundaries. Later, this method was used in solving problems in fluid and solids mechanics Johnson (1996), Colagrossi (2003). Due to the instability of Smoothed Particle Hydrodynamics (SPH) solution method monitoring, Liu *et al.* (1995)) presented a correction function labeled as the reproducing kernel practice method (RKP) solution. Generally, few studies can be found in the literatures devoted to MFree strong-form methods. This may be partly because of the MFree strong-form methods were less robust than the methods based on the weak-form, and partly because of concentrating the researches on the FEM which used weak-form.

*Corresponding author, Ph.D.
E-mail: Edalatihamed@gmail.com

ISSN: 1226-6116 (Print), 1598-6225 (Online)

Research and development of MFree methods was initiated the early 1990s. A number of weak form MFree methods were carried out by researchers can be introduced as follows: In 1994, the meshless EFG (Element Free Galerkin), in 1999, the MLPG (Meshless Local Petro-Galerkin method), in 1999, the PIM (Point Interpolation method) and in 2001, the RPIM (Radial Point Interpolation method) have been developed Liu and Gu (2005). It appears that these methods, despite their recent development and short life, will be able to be a rival for the FEMs.

Fewer researches have been used the strong from MFree solution methods in their studies. This may be, on the one hand, often unstable, not robust, and inaccurate, especially for problems with derivative boundary conditions compared with weak form and on the other hand due to more intimacy of the weak form with the FEM.

Today's plates are integral components of the industries. Due to various applications of plates in various industries, their analysis is important and essential. The behavior of plates in different static and dynamic situations can be represented by differential or integral equations. Because of the complexity of the analytical solution, a finite number of them are possible. Therefore, in order to solve these equations, along with the development of computers, scientists have approached numerical (approximation) solution methods. The latest numerical methods, is the meshless method, which is also utilized in the analysis of plates. Krysl and Belytschko Krysl (1996) have extended the element-free Galerkin (EFG) method to static analysis of thin plates and shells. In their work, the essential boundary conditions are enforced by a method of Lagrange multipliers. An EFG method has also been formulated for modal analyses of Euler–Bernoulli beams and Kirchhoff plates Ouatouati (1999), buckling problems of thin plates (Liu 2002) as well as composite laminates Chen (2003). In those works, the essential boundary conditions are imposed using orthogonal transform techniques. The determination of the stress intensity factor at the crack tip is one of the most widely used by Benchiha *et al.* (2016) methods to predict the fatigue life of aircraft structures.

Memar Ardestani *et al.* (2014) analyzed reinforced functionally graded plates under bending loads, using RKPM method. The analysis of piezoelectric circular plates by the MLPG method was carried out by Sladek *et al.* (2013). Liew et al. proposed a review of meshless methods for laminated and functionally graded plates and shells Liew *et al.* (2011). Sladek *et al*. (2007) in their research analyzed the plates under both harmonic dynamic and impact loads by using MLPG method, using this numerical method thermal analysis of plates based on the Mindlin theory have been carried out by Sladek *et al.* (2008) . In addition, thick sheets analysis with the help of local integration method Sladek *et al.* (2007),analysis of FGM composite plates Based on classical theory using element free methods And making comparison of numerical methods in bending the plates could be noticed Sladek *et al.* (2014). A state space differential reproducing kernel (DRK) method was developed by Wu and Liu (2016) for the three-dimensional (3D) analysis of functionally graded material (FGM) axisymmetric circular plates with simply-supported and clamped edges. Hadji *et al.* (2016) investigated the response of functionally graded ceramic-metal plates. The dynamic analysis of a transversely isotropic thin plate was presented by Fadodun *et al*. (2017).

In this paper, the MLPG meshless method is utilized to analyze plates with different geometries due to demonstrate the accuracyof the results. The obtained results will be compared with available analytical and finite element solutions. Using a set of mappings, composite plates of various shapes are transformed into a standard rectangular shape and then through MLPG method, they are analyzed.

In MLPG Method, due to the lack of Kronecker delta properties approximation function, and because of the nature of function system in node by node form, it is possible that the boundary conditions be directly applied. By the usage of MFree methods in classical plates, each node only has one movement variable in the direction of perpendicular axis and therefore applying two boundary conditions simultaneously into one node, is not possible. Hence, the usage of adjacent boundary conditions is discussed in this paper.

2. MLS shape function

In the MLPG method, the MLS approximation function is used. This function was introduced in 1993 with sum of the series as a function of x. In this function, a variable such as $w(x)$ in the domain Ω at point x is expressed as following (Lancaster 1981)

$$w^h(x)=\sum_{j=1}^{m} p_j(x)a_j(x)=P^T(x)a(x) \qquad (1)$$

where $P(x)$ is the basic function and m is the number of basic functions. The function $P(x)$ is quadratic polynomial basis made from Pascal's triangle to satisfy the minimum requirements. $a(x)$ is the vector of coefficients as

$$a^T(x)=\{a_1(x) \quad a_2(x) \quad \dots \quad a_m(x)\} \qquad (2)$$

Note that the vector of unknown coefficients $a(x)$ in Eq. (2) is a function of x. These coefficients are obtained by minimizing the following function

$$J=\sum_{i=1}^{n}\hat{W}(x-x_i)\left[P^T(x_i)a(x)-u_i\right]^2 \qquad (3)$$

Eq. (3) is called weighted residual equation, in which n is number of nodes within the local domain of an arbitrary point x, $\hat{W}(x-x_i)\neq 0$ is the weight function and u_i is the value of u in $x=x_i$. It is worth mentioning that the number of nodes n used in MLS approximation is often more than the number of unknown variables m, therefore approximation function $w^h(x)$ does not pass through all nodes. The stability equation of J with respect to $a(x)$ gives

$$\frac{\partial J}{\partial a}=0 \tag{4}$$

Simplifying above equation gives the following system equations

$$A(x)a(x)=B(x)U_s \tag{5}$$

$$U_s=\{u_1 \quad u_2 \quad \dots \quad u_n\}^T \tag{6}$$

Where U_s is the vector variable nodes within the local domain and $A(x)$ is called the weighted moment matrix which can be expressed as follows

$$A(x)=\sum_{i=1}^{n}W_i(x)P(x_i)P^T(x_i) \tag{7}$$

$$W_i(x)=\hat{W}(x-x_i) \tag{8}$$

The $B(x)$ matrix is defined in Eq. (5) as following

$$B(x)=[\hat{W}_1(x)P(x_1) \quad \hat{W}_2(x)P(x_2) \quad \dots \quad \hat{W}_n(x)P(x_n)] \tag{9}$$

solving Eq. (5) for $A(x)$ and substituting in Eq. (1), the following equations are obtained

$$u^h(x)=\sum_{i=1}^{n}\phi_i(x)u_i=\phi^T(x)U_s \tag{10}$$

Here, $\phi(x)$ is vector of MLS shape functions for n nodes within a local area of an arbitrary point x that can be calculated as follows

$$\emptyset^T(x)=\{\emptyset_1(x) \quad \emptyset_2(x) \quad \dots \quad \emptyset_n(x)\}_{(1\times n)}=P^T(x)A^{-1}(x)B(x) \tag{11}$$

3. Plate theories

Consider a plate with the domain Ω showed in Fig. (1). The values of displacement along the *x*, *y* and *z* directions are indicated as *u*, *v*, *w*.

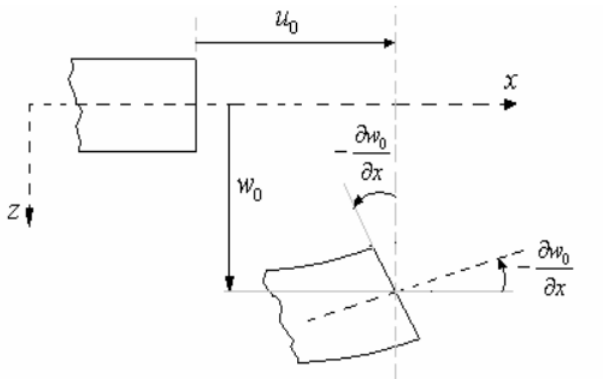

Fig. 1 Configuration of a plate and its coordinate system

Based on the Kirchhoff assumptions the displacement components in terms of z are given as

$$\mathbf{u}=\begin{Bmatrix}u\\v\\w\end{Bmatrix}=\begin{Bmatrix}-z\dfrac{\partial}{\partial x}\\-z\dfrac{\partial}{\partial y}\\1\end{Bmatrix}w=\mathbf{L}_{\mathbf{u}}w \tag{12}$$

The strain-displacement equation is expressed as

$$\varepsilon=\begin{Bmatrix}\varepsilon_{xx}\\\varepsilon_{yy}\\\gamma_{xy}\end{Bmatrix}=z\begin{bmatrix}-\dfrac{\partial^2}{\partial x^2}\\-\dfrac{\partial^2}{\partial y^2}\\-2\dfrac{\partial^2}{\partial x\,\partial y}\end{bmatrix}w=zL_dw \tag{13}$$

Applying Eqs. (12) and (13) into the constitutive equation of the material, the stress components in terms of displacement can be expressed as follows

$$\sigma=\begin{Bmatrix}\sigma_{xx}\\\sigma_{yy}\\\sigma_{xy}\end{Bmatrix}=zcL_dw \tag{14}$$

For an isotropic material, the stiffness matrix is reduced as (Krysl 1996)

$$c=\frac{E}{(1-\vartheta^2)}\begin{bmatrix}1&\nu&0\\\vartheta&1&0\\0&0&(1-\vartheta)/2\end{bmatrix} \tag{15}$$

Which can be used for wide range of composites. In this study, the material is assumed to be orthotropic. In plane stress condition, the stiffness matrix can be expressed as follows (Kaw 2006)

$$\bar{Q}=\begin{bmatrix}\bar{Q}_{11}&\bar{Q}_{12}&\bar{Q}_{16}\\\bar{Q}_{16}&\bar{Q}_{22}&\bar{Q}_{26}\\\bar{Q}_{16}&\bar{Q}_{26}&\bar{Q}_{66}\end{bmatrix}\text{?} \tag{16}$$

Where $\overline{Q_{ij}}$ is calculated by using the following transfer matrix

$$T=\begin{bmatrix}cos^2\theta&sin^2\theta&2sin\theta?cos\theta\\sin^2\theta&cos^2\theta&-2sin\theta?cos\theta\\-sin\theta\text{?}cos\theta&sin\theta\,cos\theta&cos^2\theta-sin^2\theta\end{bmatrix} \tag{17}$$

$$R = \begin{bmatrix} 1 & 0 & 0 \\ 0 & 1 & 0 \\ 0 & 0 & 2 \end{bmatrix} \tag{18}$$

$$\left[\bar{Q}\right] = \left[T\right]^{-1}\left[Q\right]\left[R\right]\left[T\right]\left[R\right]^{-1} \tag{19}$$

In above equations, θ is fiber twisting angle, Q_{ij} are the stiffness matrix components in the original coordinate system (in the direction of the fibers and perpendicular with the fibers). Based on the mechanical properties of the plate in the principal directions, this matrix is expressed as follows

$$\left[Q\right] = \begin{bmatrix} Q_{11} & Q_{12} & 0 \\ Q_{12} & Q_{22} & 0 \\ 0 & 0 & Q_{66} \end{bmatrix} \tag{20}$$

In which

$$Q_{11} = \frac{E_1}{1-\vartheta_{12}\vartheta_{21}} \qquad Q_{12} = \frac{\vartheta_{12}E_2}{1-\vartheta_{12}\vartheta_{21}}$$

$$Q_{22} = \frac{E_2}{1-\vartheta_{12}\vartheta_{21}} \qquad Q_{66} = G_{12} \tag{21}$$

$$\vartheta_{12}E_2 = \vartheta_{21}E_1$$

Based on the given relations between equations, it can be observed that the stress equations are linear functions in accordance with the vertical distance to the middle plate (z). Herein, two parameters of pseudo strain and pseudo stress are defined as follows which are constant in plate cross section and independent of z value.

$$\varepsilon_p = L_d w \tag{22}$$

$$\sigma_p = D\varepsilon_p = DL_d w \tag{23}$$

The matrix D in isotropic and composite materials can be expressed as follows, respectively

$$D = \frac{Eh^3}{12\left(1-\vartheta^2\right)}\begin{bmatrix} 1 & \vartheta & 0 \\ \vartheta & 1 & 0 \\ 0 & 0 & \left(1-\vartheta\right)/2 \end{bmatrix} \tag{24}$$

$$D_{ij} = \frac{1}{3}\sum_{k=1}^{n_l}\left[\bar{Q}_{ij}\right]_k \left[z_k^{\,3} - z_{k-1}^{\,3}\right] \tag{25}$$

4. Enforcing essential boundary conditions

The boundary conditions of a plate are expressed as follows

$$u_\Gamma = u_b \qquad \Gamma_u = \Gamma_w \cup \Gamma_\theta \tag{26}$$

Where u_b is a vector involving transverse and rotation displacement on the boundaries consisting of essential conditions in plates is defined as follows

$$u_b = L_b W \tag{27}$$

In this equation, $u_b = L_b W$ is differential operator vector which can be defined as follows for various support conditions:

For fixed support

$$L_b = \begin{bmatrix} 1 \\ \dfrac{\partial}{\partial n} \end{bmatrix} \tag{28}$$

For simply supports

$$L_b = \begin{bmatrix} 1 \\ 0 \end{bmatrix} \tag{29}$$

5. MLPG method

The MLS approximation function has been widely used in the MLPG method. MLPG method was presented by Atlury and Shen in 1998 (Atluri 1998). This method is still being used and developed by other researchers in solving elasto-static problems, elasto-dynamic problems, analysis of thin and thick beams, analysis of plates and shells, fluid flow, fracture mechanics, etc.

The element free Galerkin method (EFG) is based on general Galerkin weak form process, in which a background gridding is required for the numerical integration; hence, this solution methodology is not thoroughly meshless. To avoid the complete gridding of the domain of the problem, the local weak form MLPG method was presented. In this approach, local quadrature domains of each node are used for numerical integration.

As mentioned above, the MLS shape functions are used in this method and due to the fact that this function does not have Kronecker's delta approximation property, it is therefore required to apply some measures to enforce boundary essential conditions and here direct method is used.

In the MLPG method, the governing equations are expressed using a weak form of the weighted residuals.

$$\int_{\Omega_s} \hat{V}\left(\sigma_{ij,j} + b_i\right)d\Omega - \alpha \int_{qu} \hat{V}\left(w_i + \overline{w_j}\right)d\Gamma = 0 \tag{30}$$

Where $\hat{V}$ is weight or test function, the second integral is for satisfying essential boundary conditions , Ω_q is the problem domain, Γ_{qu} is the area on boundary with

essential boundary conditions and α is the penalty factor. If the penalty method is used in enforcing the boundary conditions, the governing equation will be presented as Eq. (30), but since direct method is used in this study, the governing equation is expressed as following

$$\int_{\Omega_s} \hat{V}\left(\sigma_{ij,j} + b_i\right) d\Omega = 0 \tag{31}$$

Substituting Eqs. (23) and (27) in Eq. (31) and simplifying the governing equations in MLPG method yields

$$\int_{\Omega_q} \hat{V}\left(D\nabla^4 w - b\right) d\Omega = 0 \tag{32}$$

Using the approximation functions (Eq. (1)) in the governing equations (Eq. (32)) and simplifying by means of parts by part integration technique, the matrix form of the equilibrium equations is achieved as follows

$$[K]\{W\} = \{F\} \tag{33}$$

[K] is stiffness matrix, [W] is displacement vector and [F] is the vector of force. Each of the matrices can be calculated as follows

$$[K] = [K]_\Omega + [K]_i \tag{34}$$

$$[K_{ij}]_\Omega = \int_{\Omega_s} \left\{ [\hat{V}_{i,xx} \quad \hat{V}_{i,yy} \quad \hat{V}_{i,xy}] \begin{bmatrix} D_{11} & D_{12} & 0 \\ D_{12} & D_{22} & 0 \\ 0 & 0 & D_{66} \end{bmatrix} \begin{bmatrix} \emptyset_{j,xx} \\ \emptyset_{j,yy} \\ \emptyset_{j,xy} \end{bmatrix} \right\} d\Omega \tag{35}$$

$$\left[K_{ij}\right]_i = \int_{\Gamma_{si}} \left[B_{ij}\right] d\Gamma \tag{36}$$

$$\begin{aligned} \left[B_{ij}\right] = & \hat{V}_i \left[\left(D_{11}\varnothing_{j,xxx} + \left(D_{12} + 2D_{66}\right)\varnothing_{j,xyy}\right) n_x \right. \\ & \left. + \left(D_{22}\varnothing_{j,yyy} + \left(D_{12} + 2D_{66}\right)\varnothing_{j,xxy}\right) n_y \right] \\ & - \hat{V}_{i,x} \left[\left(D_{11}\varnothing_{j,xx} + D_{12}\varnothing_{j,yy}\right) n_x + 2D_{66}\varnothing_{j,xy} n_y \right] \\ & - \hat{V}_{i,y} \left[2D_{66}\varnothing_{j,xy} n_x + \left(D_{12}\varnothing_{j,xx} + D_{22}\varnothing_{j,yy}\right) n_y \right] \end{aligned} \tag{37}$$

$$f_i = \int_{\Omega_s} \hat{V}_i f d\Omega - \int_{\Gamma_{qu}} \alpha_1 \hat{V}_i \bar{w} d\Gamma - \int_{\Gamma_{qu}} \alpha_2 \hat{V}_{i,n} \bar{\theta} d\Gamma \tag{38}$$

Obviously it can be seen that the stiffness matrix [K] is bounded and asymmetric whereas in the EFG method, the stiffness matrix is symmetric; therefore the computational cost in this method is much more.

Since there is one unknown variable in each node, two boundary conditions cannot be simultaneously enforced to each node. In order to enforce boundary conditions, the neighborhood boundary condition is implemented. This modification for enforcing boundary conditions is introduced and applied in this study for MLPG method for the first time.

To apply the neighborhood boundary conditions some new nodes are located in the neighborhood of bounder nodes in ε distance where ε is approximately equal to one millionth of the average distance between nodes. Later the displacement boundary conditions are enforced to nodes on the boundary and the derivational displacement conditions are enforced to the adjacent nodes.

The governing equations for each node on the boundary and each adjacent node are as follows

$$w_i = \begin{bmatrix} \phi_1 & \cdots & \phi_n \end{bmatrix} \begin{bmatrix} w_1 \\ \vdots \\ w_n \end{bmatrix} = \overline{w_i} \tag{39}$$

$$\frac{\partial w_i}{\partial n} = \begin{bmatrix} \frac{\partial \phi_1}{\partial n} & \cdots & \frac{\partial \phi_n}{\partial n} \end{bmatrix} \begin{bmatrix} w_1 \\ \vdots \\ w_n \end{bmatrix} = \frac{\partial \overline{w_i}}{\partial n} \tag{40}$$

6. Geometry mapping

As stated before, the governing differential equations and boundary conditions equations are given in Cartesian coordinates for plates. The plates with curved form geometry cannot be easily analyzed. Therefore, the curved line environment into rectangular shape environment is mapped. This mapping is often performed by shape functions which are mostly used in finite element. The accuracy of the mapping is increased by increasing the order of the shape function. Hence, third order shape functions are utilized here as shu (2000)

$$x = \sum_{i=1}^{12} N_i(\xi, \eta).x_i \tag{41}$$

$$y = \sum_{i=1}^{12} N_i(\xi, \eta).y_i \tag{42}$$

$$N_i = \frac{1}{32}\left(1+\xi_i\xi\right)\left(1+\eta_i\eta\right)\left[9\left(\xi^2+\eta^2\right)-10\right] \quad i = 1,2,3,4 \tag{43}$$

$$N_i = \frac{9}{32}\left(1-\xi^2\right)\left(1+\eta_i\eta\right)\left(1+9\xi_i\xi\right) \quad i = 5,6,7,8 \tag{44}$$

$$N_i = \frac{9}{32}\left(1-\eta^2\right)\left(1+\xi_i\xi\right)\left(1+9\eta_i\eta\right) \qquad (45)$$
$$i = 9,10,11,12$$

7. Numerical results

In this section, the accuracy and reliability of the present method are evaluated by some examples. To use the MLPG method a comprehensive code has been written by MATLAB Software. The obtained results by the present method will be compared with analytical solution and FEMs to verify the results.

To demonstrate the reliability of the written code, a rectangular plate is studied with the specified demonstrated in Table (1) in which the analytical solutions are available.

The deviations of the results with the exact solution are examined by following function

$$Error = \frac{\varepsilon_{exat} - \varepsilon_p}{\varepsilon_{exat}} \times 100 \qquad (46)$$

7.1 Thin square plate with simple and fixed support under distributed load

A 0.01m thin square SSSS support plate under distributed force of $100\frac{N}{m^2}$ is considered. The dimensionless formula for deflection state is considered as follows Liu (2002)

$$\bar{W} = \frac{W_{max} D}{qb^4} \qquad (47)$$

Where q is the force, b is plate dimension and D is bending stiffness of the plate which is defined as

$$D = \frac{Eh^3}{12\left(1-\vartheta^2\right)} \qquad (48)$$

The results of the transverse deflection are shown in Table 2. In exact solution of this example case, which has been conducted by Timoshenko, the quantity of dimensionless deflection is equal to 0.00406 Timoshenko (1959) while the result of the FEM for this problem is 0.00405 Zienkiewicz(2000).

Table 1 Geometrical and mechanical characteristics

Dimension plates(m)	0.6×0.6
Young's modulus(GPa)	200
Poisson coefficient	0.3
Thickness(m)	0.01

Table 2 Dimensionless deflection of thin square plate with simply support under constant load

Number of nodes	10×10	13×13	15×15	18×18	Abaqus 900 linear element	Abaqus 900 nonlinear element
Dimensionless deflection	0.0037	0.00417	0.00419	0.00403	0.00408	0.00410
Error	8.8%	2.7%	3.2%	0.7%	0.5%	0.98%

Table 3 Dimensionless deflection of thin square plate with fix support under constant load

Number of nodes	10×10	13×13	15×15	17×17	Abaqus 900 linear element	Abaqus 900 nonlinear element
Dimensionless deflection	0.00130	0.00128	0.00127	0.00127	0.00125	0.00126
Error	3.1%	1.5%	0.7%	0.7%	0.5%	0.98%

Table 3 exhibits the results of the mentioned plate whose four sides are under fixed supports. The exact solution of this example was conducted by Timoshenko(1995) and the quantity of dimensionless deflection is equal to 0.00126. while in FEM solution, this value is equal to 0.001283 Zienkiewicz (2000). As can be seen, the accuracy of the results of the MLPG approach is more than the finite element results.

Modified forms of a square plate in two simple and fixed supports positions are respectively illustrated in Figs. 2 and 3. As can be seen in these figures, problem domain and the form modification for plate is only shown by nodes. Paying attention to the type of nodes deformation, the effects of boundary conditions on the solution results could be seen.

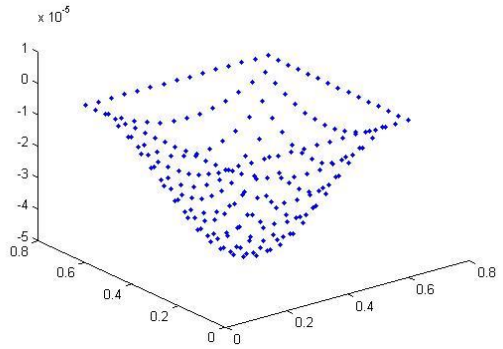

Fig. 2 Modified form of a square plate with simple support under constant distributed latitudinal force

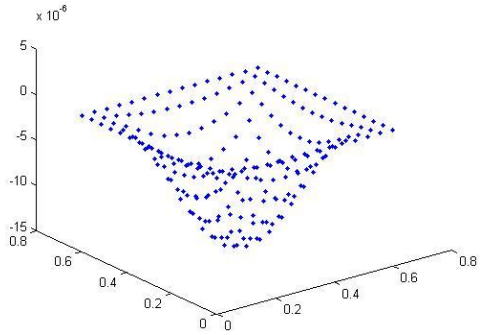

Fig. 3 Modified form of a square plate with cantilever support under constant distributed latitudinal force

Fig. 4 shows Von Misses pseudo stress σ_{vp} distribution calculated from Eq. (49) at middle line of the plates ($x = 0.3$) under both simply and clamp supports. By multiplying the vertical distance of any points to the meddle plane of the plate, von Misses stress at that point can be computed as follows

$$\sigma_{vp} = \sqrt{\left(\sigma_{xp}^2 + \sigma_{yp}^2 - \sigma_{xp}\sigma_{yp}\right)} \tag{49}$$

7.2 Thin rectangular plate with simple and fixed supports under distributed load

The rectangular plate with mechanical properties introduced in Table 1, is investigated here. The results are compared with the analytical solution outputs as stated in Timoshenko (1959). Also, Tables 4 and 5 show the displacement of a rectangular plate obtained by Abaqus Software with 15 × 15 nodes under a distributed transverse load (100 N/m^2) with simply and fixed supports, respectively.

Fig. 5 illustrates the Von Misses pseudo stress (σ_{vp}) distribution along the line $b/2 = 0.3$ (the line that divides the plate into two parts) in both simply support and fixed boundary condition. It is observed that in the case of simply and fixed supports, critical point is located on the plate center and plate bounders, respectively.

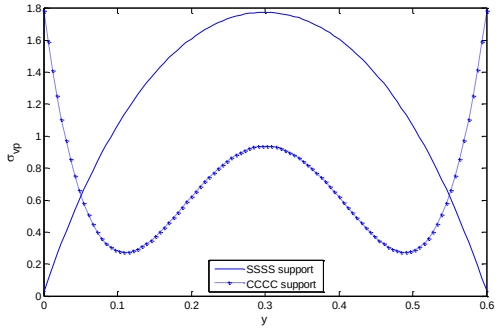

Fig. 4 Von Misses pseudo stress

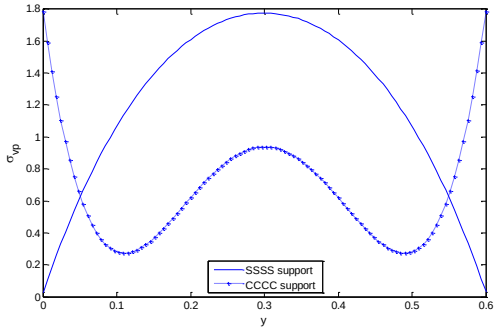

(a) SSSS support

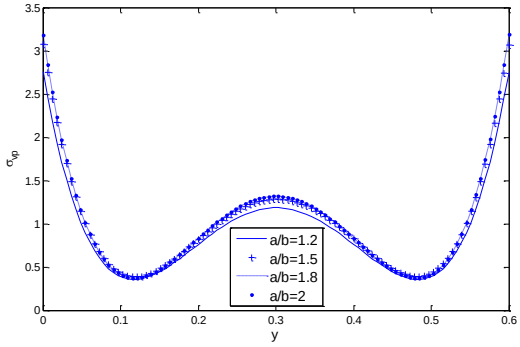

Fig. 5 Von Misses pseudo stress of thin rectangular plate under constant load

Table 4 Dimensionless deflections of thin rectangular plate simply support under constant load

length /width	1.5	2	3	4
MLPG	0.00772	0.01014	0.01225	0.01289
Reference	0.00772	0.01013	0.01223	0.01282
Abaqus 900 linear element	0.00770	0.01008	0.01212	0.01268

Table 5 Dimensionless deflections of thin rectangular plate fix support under constant load

length /width	1.2	1.5	1.8	2
MLPG	0.00175	0.00222	0.00249	0.00260
Reference	0.00172	0.00220	0.00245	0.00254
Abaqus 900 linear element	0.001717	0.00216	0.00235	0.00249

7.3 Thin circular plate with simple and fixed supports under distributed load

Consider a circular thin plate with 1 m radius under 100N/m^2 uniformly distributed load. The obtained results have been become dimensionless though local Petro

Galerkin meshless method, based on the following equation

$$\alpha = \frac{w_{max} Eh^3}{pa^4} \quad (50)$$

The comparison between present results and those obtained by Timoshenko (1959) reveals that high accuracy can be achieved by the usage of 15 × 15 nodes for problem domain. It is important to note that some of the observed errors are from mapping of the circular into the rectangular domain. By applying appropriate mapping, perfect precision for results can be obtained.

Figs. 6 and 7 show distribution of deformation for simple and fixed circular plates, respectively.

Fig. 8 presents Von Misses pseudo stress distribution along the diameter of the circular plate under the force constant for both simply and fixed supports. In the case of a fixed support the magnitudes of stress is more than simply support ones. The critical point of simply support plate is located in the near of supports, whereas for fixed support, it is located in the plate center.

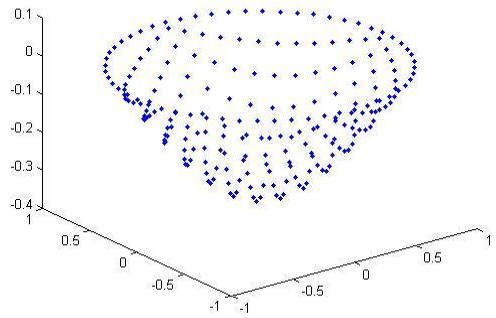

Fig. 6 Modified form of circular plate with simple support under constant latitudinal distributed force

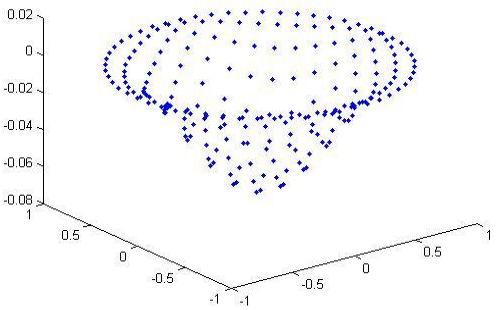

Fig. 7 Modified form of a circular plate with cantilever support under constant latitudinal distributed force

Table 6 Dimensionless displacement of circular plate

	MLPG Method			Reference Timoshenko (1959)	*Abaqus*	*Abaqus*
Number of nodes	10×10	13×13	15×15		925 linear	925 nonlinear
simply support	0.05544	0.06241	0.06212	0.06370	0.0635	0.0637
fixed support	0.01428	0.01549	0.01553	0.01562	0.0156	0.0156

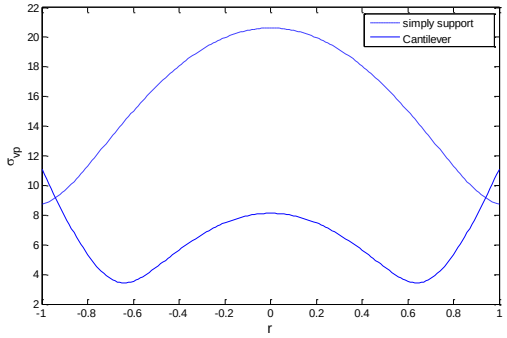

Fig. 8 Von Misses pseudo stress of thin circular plate under constant load

7.4 Elliptical shaped thin plate with simple and fixed supports under distributed load

An Elliptical shaped plate with mechanical properties of table 1 is analyzed and by the usage of Eq. (50), the dimensionless form of obtained results from the software can be derived. The dimensionless displacement for simply and fixed support, using 20×20 nodes for the problem domain are exhibited in Tables 7 and 8, respectively. Besides, Figs. 9 and 10 show the modified form of oval plates in specific state of a/b=2 for two different supporting conditions.

Table 7 Dimensionless displacement of oval plate with joint support

a/b	1.5	2	3	4
MLPG	1.23	1.53	1.83	1.98
Abaqus	1.25	1.55	1.856	2.00
Timoshenko (1959)	1.26	1.58	1.88	2.02

Table 8 Dimensionless displacement of oval plate with fixed support

a/b	1.5	2	3	4
MLPG	0.2958	0.3443	0.3983	0.4236
Abaqus	0.304	0.3697	0.4177	0.434
Timoshenko (1959)	0.3046	0.3701	0.4188	0.4352

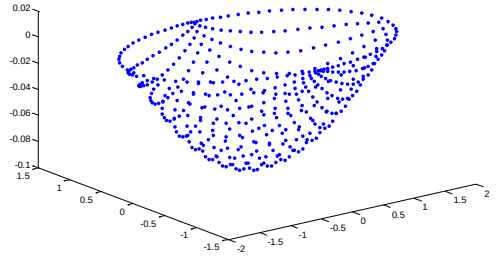

Fig. 9 Deformed shape of oval plate with simply support under uniform latitudinal distributed load

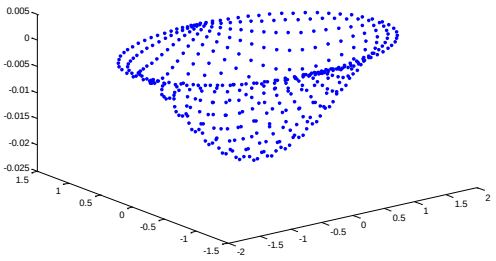

Fig. 10 Deformed shape oval plate with cantilever support under constant distributed latitudinal distributed force

Fig. 11 shows the Von Misses pseudo stress (σ_{vp}) distribution along Small diameter in both simply and fixed support. It can be observed that the maximum value of the stress takes place in the center of the plate and near the supports for the simply and fixed support boundary conditions, respectively.

7.5 Ortho-tropic rectangular and square plates under distributed load

Here, the analysis and comparison of behavior of the orthotropic plates under uniformly distributed load for simply and fixed support conditions have been carried out. Table 9 presents the results of the orthotropic plate, considering properties of $E_1 = 25E_2, G_{12} = 0.5E_2$, $\vartheta_{12} = 0.25$. The exact solution of this case is given by Reddy (2003) and dimensionless deflection has been obtained as 0.6497 .

The results for finite element for this problem in two boundary conditions of using conforming and non-conforming elements are calculated as 0.6551 and 0.6535, respectively. It is observed that the error of the finite element results is 2.5% Reddy (2003). In Fig. 12 compare the results of the analytical solution and Galerkin meshless method in a composite rectangular four-layer plate with the layout of (0/90/90/0) for which the properties of the layers are$E_1 = 25E_2$, $G_{12} = 0.5E_2$, $\vartheta_{12} = 0.25$.

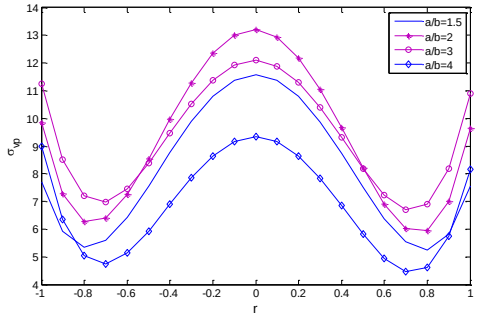

(a) Clamp support

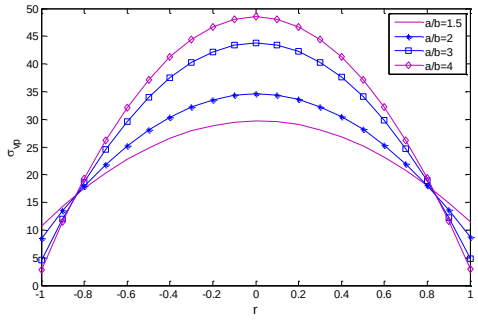

(b) Simply support

Fig. 11 Von Misses pseudo stress of thin Elliptical plate under constant load

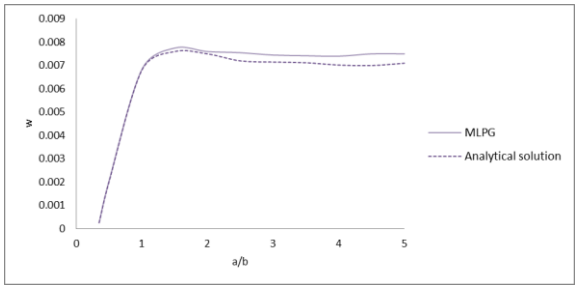

Fig. 12 Dimensionless displacement of composite rectangular plate with fixed support

Table 9 Dimensionless deflection of thin orthotropic cubic plate with simple support under constant load

Number of nodes	10×10	13×13	15×15	17×17
Dimensionless deflection	0.6602	0.6547	0.6313	0.6577
Error	0.6602	0.6547	0.6313	0.6577

7.6 Orthotropic circular plate

The comparison of the displacement in an orthotropic circular plate with properties of $E_1 = 131\text{GPa}, E_2 = 13\text{GPa}, G_{12} = 6.4\text{GPa}, \vartheta_{12} = 0.34$, and dimensions of $R = 1m?$ $h = 12mm?$ under distributed force of 100N/m^2 for both the meshless Galerkin and FEMs is presented Rao (1994).

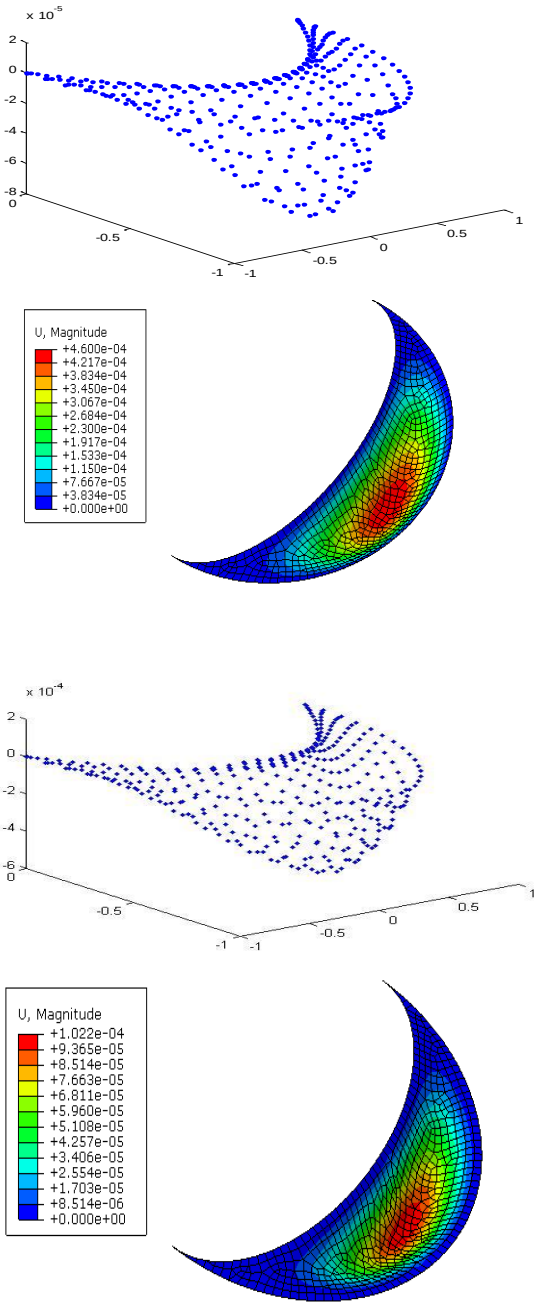

Fig. 12 Deformed Crescent shape of oval plate

Table 10 displacement in the center of circular plate (in millimeters)

	Solution method MLPG			Rao (1994)
Number of nodes	10×10	13×13	15×15	
Fixed support	1.3	1.4	1.4	1.84

Table 11 maximum displacement in the Crescent-shaped plate

Type plates	Type support	EFG 441 node	*Abaqus* 1088 element
isotropic	simply support	0.483	0.46
	Cantilever	0.098	0.102
orthotropic	simply support	0.705	0.898
	Cantilever	0.14	0.18

7.7 Crescent-shaped plate isotropic and orthotropic

Given the capabilities of the different forms analysis the crescent-shaped plate of the hitting of a circle with a radius of one meter and a geometric ellipse equation is $x^2+4y^2=1$ is created, Under the uniform force $100\frac{N}{m^2}$ in two the simply support and fixed studied. Table 11 shows that the results for both isotropic and orthotropic plate are consistent with the mechanical characteristics of the previous example. Fig. (12) compares a modified form of sheets with the computer programs and Abaqus software.

8. Conclusions

Analysis of thin isotropic and orthotropic plates with various geometries and boundary conditions is proposed, based on the meshless Galerkin method. As can be realized from the results, the outputs are relatively stable with the number of nodes and this is the benefit of weak form method. Also, element categorization of the solution domain is not necessary, which is a complex process in FEM. Therefore, because there is no networking for problem domain in this method, network computations are removed. In comparison with FEM, it also has advantages such as more accurate results, faster convergence and fewer nodes in comparison with the number of elements.

In the computer code, using adjacency boundary conditions instead of penalty method gives more accurate results whereas in the penalty method the error penalty coefficient is estimated by trial and error. It needs to be mentioned that change in the distance between adjacent nodes to the node on the boundary has insignificant effect on the results accuracy.

Acknowledgements

The authors are grateful to University of Kashan for supporting this work by Grant.

References

Akgul, M., Demir, M. and Akay, A.E. (2017), "Analyzing dynamic curve widening on forest roads", *J. Forest. Res*., **28**(2), 411-417.

Atluri, S.N. and Zhu, T. (1998), "A new meshless local Petrov-Galerkin (MLPG) approach in computational mechanics", *Comput. Mech*., **22**, 117-127.

Benchiha, A., Madani, K., Touzain, S., Feaugas, X. and Ratwani, M. (2016), "Numerical analysis of the Influence of the presence of disbond region in adhesive layer on the Stress intensity factors (SIF) and crack opening displacement (COD) in plates repaired with a composite patch", *Steel Compos. Struct.*, **20**(4), 951-962.

Chen, X.L., Liu, G.R. and Lim, S.P. (2003), "An element free Galerkin method for the free vibration analysis of composite laminates of complicated shape", *Compos. Struct*., **59**(2), 279-289.

Colagrossi, A. and Landrini, M. (2003), "Numerical simulation of interfacial flows by smoothed particle hydrodynamics", *J. Comput. Phys.*, **191**(2), 448-475.

Fadodun, O.O., Borokinni, A.S., Layeni, O.P. and Akinola, A.P. (2017), "Dynamic analysis of a transversely isotropic non-classical thin plate", *Wind Struct*., **25**(1), 25-38.

Johnson, G.R., Stryk. R.A. and Beissel, S.R. (1996), "SPH for high velocity impact computations", *Comput. Method. Appl. M*., **139**(1-4), 347–373.

Hadji, L., Zouatnia, N. and Kassoul, A. (2016), "Bending analysis of FGM plates using a sinusoidal shear deformation theory", *Wind Struct*., **23**(6), 543-558.

Kaw, A.K. (2006), Mechanics of composite materials. CRC Press, *Taylor & Francis Group*.

Krysl, P. and Belytschko, T. (1996), "Analysis of thin plates by the element-free Galerkin method", *Comput. Mech*., **17**, 26-35.

Lancaster, P. and Salkauskas, K. (1981), "Surfaces generated by moving least squares methods", *Math. Comput*., **37**, 141-158.

Liew, K.M., Zhao, X. and Ferreira, A.J.M. (2011), "A review of meshless methods for laminated and functionally graded plates and shells", *Compos. Struct.*, **93**(8), 2031-2041.

Liu, G.R. (2002), "Meshfree methods-moving beyond the Finite element method", *CRC Press*.

Liu, G.R. and Gu, Y.T. (2005), An introduction to mesh free methods and their programming, Springier.

Liu, G.R., Chen, X. and Reddt, J.N. (2002), "Bucking of symmetrically laminated composite plates using the element-free Galerkin method", *Struct. Stab. Dynam*., **2**(3), 281-294.

Liu, W.K., Jun, S., Li, S., Adee, J. and Belytschko, T. (1995), "Reproducing kernel particle method for structural dynamics", *Int. J. Numer. Meth. Eng*., **38**, 1655-1679.

Memar Ardestani, M., Soltani, B. and Shams, Sh. (2014), "Analysis of functionally graded stiffened plates based on FSDT utilizing reproducing kernel particle method", *Compos. Struct.*, **112**, 231-240.

Ouatouati, A.E. and Johnson., D.A. (1999), "A new approach for numerical modal analysis using the element free method", *Int. J. Numer. Meth. Eng*., **46**, 1-27.

Sridhar, C. and Rao, K.P. (1994), "Large deformation finite element analysis of laminated circular composite plates", *Comput. Struct*., **54**, 59-64.

Reddy, J.N. (2003). Mechanics of Laminated Composite Plates and shell theory and analysis, *CRC PRESS*.

Shu, C. (2000), Differential Quadrature and Its Application in Engineering, Springer.

Sladek, J., Sladek, V., Stanak, P., Zhang, C. and Wünsche, M. (2013), "Analysis of the bending of circular piezoelectric plates with functionally graded material properties by a MLPG method", *Eng. Struct*., **47**, 81-89.

Sladek, J., Sladek, V., Krivacek, J., Wen, P.H. and Zhang, Ch. (2007), "Meshless local Petrov-Galerkin (MLPG) method for Reissner-Mindlin plates under dynamic load", *Comput. Meth. Appl.*, **196**, 2681-2691.

Sladek, J., Sladek, V., Hellmich, Ch., Eberhardsteiner, J., (2007) "Analysis of thick functionally graded plates by local integral equation method", *Communic. Numeric. Meth. Eng.*, **23**,733-754

Sladek, J., Sladek, V., Solek, P. and Wen, P.H. (2008), "Thermal bending of Reissner-Mindlin plates by the MLPG", CMES - *Comput. Meth. Appl*, **28**, 57-76.

Sladek, V., Sladek, J. and Sator, L. (2013), "Physical decomposition of thin plate bending problems and their solution by mesh-free method", *Eng. Anal. Bound.Elem*., **37**(2), 348-365.

Sator, L., Sladek, V. and Sladek, J. (2014), "Coupling effects in elastic analysis of FGM composite plates by mesh-free methods", *Compos. Struct*., **115**, 100-110.

Szafrana, Z. (2005), "Elastic analysis of thin fiber-reinforced plates", *Civil. Environ. Eng*., **12**, 231-242.

Timoshenko, S. (1959). Theory of plates and shells.

Wu, C.P. and Liu, Y.C. (2016), "A state space Meshless method for the 3D analysis of FGM axisymmetric circular plates", *Steel Compos. Struct.*, **22**(1), 203-216.

Zienkiewicz, O.C. and Taylor, R.L. (1977), The finite element method, *Taylor*.

CC